

UC Riverside

UC Riverside Previously Published Works

Title

Evidence of Neural Microstructure Abnormalities in Type I Chiari Malformation: Associations Among Fiber Tract Integrity, Pain, and Cognitive Dysfunction.

Permalink

<https://escholarship.org/uc/item/0f0650ft>

Journal

Pain Medicine, 21(10)

Authors

Allen, Philip

Rogers, Jeffrey

Lien, Mei-Ching

et al.

Publication Date

2020-10-01


DOI

10.1093/pm/pnaa094

Peer reviewed

NEUROPATHIC PAIN SECTION

Evidence of Neural Microstructure Abnormalities in Type I Chiari Malformation: Associations Among Fiber Tract Integrity, Pain, and Cognitive Dysfunction

James R. Houston , PhD,* Michelle L. Hughes, MA,[†] Ilana J. Bennett, PhD,[‡] Philip A. Allen, PhD,[†] Jeffrey M. Rogers, PhD,[§] Mei-Ching Lien, PhD,[¶] Haylie Stoltz,* Ken Sakaie, PhD,^{||} Francis Loth, PhD,** Jahangir Maleki, MD, PhD,^{††} Sarel J. Vorster, MD,^{**} and Mark G. Luciano, MD, PhD^{§§}

*Department of Psychology, Middle Tennessee State University, Murfreesboro, Tennessee; [†]Department of Psychology, University of Akron, Akron, Ohio; [‡]Department of Psychology, University of California, Riverside, California, USA; [§]Faculty of Health Sciences, University of Sydney, Sydney, Australia; [¶]School of Psychological Science, Oregon State University, Corvallis, Oregon; ^{||}Department of Diagnostic Radiology, Cleveland Clinic Foundation, Cleveland, Ohio; **Department of Mechanical Engineering, University of Akron, Akron, Ohio; ^{††}Center for Neuro-Restoration, Cleveland Clinic Foundation, Cleveland, Ohio; ^{**}Department of Neurological Surgery, Cleveland Clinic Foundation, Cleveland, Ohio; ^{§§}Department of Neurosurgery, Johns Hopkins Medical Center, Baltimore, Maryland, USA

Correspondence to: Philip A. Allen, PhD, Department of Psychology, University of Akron, Akron, OH 44325-4301, USA. Tel: (330)972-6177; Fax: (330)972-5174; E-mail: paallen@uakron.edu.

Conflict of interest: The authors declare that they have no competing interest.

Abstract

Background. Previous case–control investigations of type I Chiari malformation (CMI) have reported cognitive deficits and microstructural white matter abnormalities, as measured by diffusion tensor imaging (DTI). CMI is also typically associated with pain, including occipital headache, but the relationship between pain symptoms and microstructure is not known. **Methods.** Eighteen CMI patients and 18 adult age- and education-matched control participants underwent DTI, were tested using digit symbol coding and digit span tasks, and completed a self-report measure of chronic pain. Tissue microstructure indices were used to examine microstructural abnormalities in CMI as compared with healthy controls. Group differences in DTI parameters were then reassessed after controlling for self-reported pain. Finally, DTI parameters were correlated with performance on the digit symbol coding and digit span tasks within each group. **Results.** CMI patients exhibited greater fractional anisotropy (FA), lower radial diffusivity, and lower mean diffusivity in multiple brain regions compared with controls in diffuse white matter regions. Group differences no longer existed after controlling for self-reported pain. A significant correlation between FA and the Repeatable Battery for the Assessment of Neuropsychological Status coding performance was observed for controls but not for the CMI group. **Conclusions.** Diffuse microstructural abnormalities appear to be a feature of CMI, manifesting predominantly as greater FA and less diffusivity on DTI sequences. These white matter changes are associated with the subjective pain experience of CMI patients and may reflect reactivity to neuroinflammatory responses. However, this hypothesis will require further deliberate testing in future studies.

Key Words: Chiari Malformation; Cerebellar Disease; Chronic Pain; Diffusion Tensor Imaging; Brain Morphology

Introduction

Chiari malformation type I (CMI) is defined as cerebellar tonsillar herniation through the foramen magnum of at least five millimeters. Symptoms of CMI include

headache, paresthesia, neck pain, and cognitive dysfunction [1,2]. Approximately 0.1% of the population is affected by this neurological dysmorphism [3–5]. However, the relationship between the structural neuropathology

of the condition and the constellation of common physical, cognitive, and affective symptoms is not well understood.

Fiber-Tract Integrity and Chiari Malformation

Diffusion tensor imaging (DTI) has become a useful tool for investigating *in vivo* microstructural integrity of white matter within the brain [6,7]. In white matter, the coherent organization of bundled axons of similar orientation results in parallel diffusion of water along the axon bundles. However, in cases of axonal degeneration and/or demyelination, there is a disruption of the diffusion [8]. Typical microstructure parameters used to index tissue integrity are fractional anisotropy (FA), mean diffusivity (MD), axial diffusivity (AD), and radial diffusivity (RD). Changes in these parameters are associated with pathology and functional deficits [9–13].

DTI has been used to assess brain-wide effects on white matter integrity in individuals with CMI. For example, compared with healthy controls, CMI patients have exhibited lower FA and higher MD in the genu and splenium of the corpus callosum [14], higher FA in the anterior brainstem [15,16], and higher AD in the posterior limb of the internal capsule, genu, pons-medial lemniscus, and brainstem, as well as increases in RD for the middle cerebellar peduncle [16]. Krishna et al. [15] also observed that CMI patients showed significant decreases in brainstem FA after surgery, increasing space in the posterior cranial fossa and alleviating pressure on the spinal cord (i.e., decompressive suboccipital craniectomy and cervical laminectomy). The authors argued that evidence of greater FA values in their clinical sample before surgery were a consequence of greater fiber compression, leading to increased diffusion restriction (for a similar argument applied to hydrocephalus, see Assaf et al. [17]). Given the accumulating evidence of DTI abnormalities in CMI, an examination of the relationship between symptoms and cerebral microstructure is timely.

Pain Effects in Chiari Malformation Type I

Chronic pain is the most common symptom of CMI. CMI patients frequently report self-rated pain levels similar to patients with chronic pain syndromes such as fibromyalgia, migraine headache, low back pain, and diabetic peripheral neuropathy [18–20]. The pathophysiology of CMI-related dysfunction extends structurally and functionally far beyond the ectopic cerebellar tonsils. As such, the structural vicinity of the brainstem and its complex fiber pathways is exposed to microtrauma associated with tonsillar herniation and tissue pulsatility across the foramen magnum [15]. The prevalence of multiple brain stem-related sensory symptoms (e.g., pain, dizziness, etc.) points to the functional significance of this region in CMI. Chronic pain in CMI is associated with increases in pain sensitization and disruption of top-down pain modulation, which have been implicated in

the generation and maintenance of mental health problems [20] and cognitive deficits [21,22] that also frequently manifest in CMI. Thus, in the present study, a secondary goal is to determine whether CMI-related microstructural abnormalities are related to concomitant chronic pain experienced by CMI patients.

Cognitive Effects in Chiari Malformation Type I

There is growing evidence that individuals diagnosed with CMI show cognitive deficits on experimental tasks and on standardized neuropsychological assessments [19,23–26]. However, there is a lack of consensus as to the typical cognitive profile of CMI. Points of difference include whether the condition is characterized by general decline in overall cognitive status or focal change in discrete cognitive domains [27]. In addition, there is growing evidence that pain symptoms may account for many of the cognitive deficits observed in CMI [19,21]. Of note, attention deficits are among the most robust findings, and these deficits also tend to remain significant when controlling for self-reported pain [19].

The Present Study

In sum, white matter abnormalities are commonly reported in CMI, although it remains unclear which areas of the brain are most susceptible and which DTI metrics are most sensitive. A single study has shown that DTI measures are associated with cognitive deficits in CMI [14], and further investigation in an independent sample controlling for pain symptoms is needed. Furthermore, the relationship between pain symptoms and DTI findings remains unexplained. The aim of the current study was therefore to collect DTI, cognitive, and pain data prospectively from a sample of CMI patients and matched healthy controls. It was hypothesized 1) that CMI-related differences in DTI metrics of anisotropy and diffusivity would be observed [14–16], 2) that group differences in DTI metrics would attenuate after controlling for self-reported chronic pain, 3) that CMI patients would exhibit performance deficits on neuropsychological tests thought to underlie attention [19], and 4) that CMI deficits in attention would be associated with white matter integrity as measured by DTI.

Methods

Participants

CMI patients and age-, sex-, and education-matched controls were recruited for the study. CMI patients were diagnosed by a neurosurgeon specializing in the surgical treatment of CMI (either MGL or SV) and recruited while undergoing presurgical consultation. Healthy controls were recruited from a university population and the local community via flyers and word of mouth. Individuals using opioid-based pain medications were

excluded from the study. All participants received \$100 for their participation.

Procedure

Participants completed assessment and imaging protocols as part of a larger research project [19,28]. Magnetic resonance imaging (MRI) scans and neuropsychological assessments were completed separately, typically within one week of each other. All participants provided informed consent, and this project was approved by the local institutional review boards of the University of Akron and the Cleveland Clinic. The neuropsychological assessment took place on the campus of the University of Akron, in a well-lit and noise-dampened room, under the guidance of a member of the research team trained in neuropsychological assessment (JRH). Imaging was conducted presurgically for all participants, and the Repeatable Battery for the Assessment of Neuropsychological Status (RBANS) neuropsychological assessment was administered presurgically for 16 of the 18 CMI patients. Assessments were conducted for the remaining two participants approximately three months after surgery to avoid postsurgery complications and surgery-related pain. As the performance of these participants on the RBANS and self-report scales did not serve as outliers relative to the other 16 CMI patients, results were interpreted for the full sample of 18 CMI patients and matched controls.

Self-report and Cognitive Measures

All participants completed a measure of self-reported chronic pain, the short-form McGill Pain Questionnaire (MPQ) [29]. MPQ scores comprise 15 experience ratings of pain on a Likert-type scale (0 = none to 5 = worst possible). Participants also completed the Chiari Symptom Profile (CSP). The CSP is a Chiari-specific scale that assesses aspects of the disease and treatment outcomes using 57 items on a 0–4 scale [30]. Higher scores reflect more significant disability.

Digit symbol coding and digit span subtests from the RBANS assessment were administered [31,32]. The coding subtest is a measure of processing speed; the digit span subtest is a measure of short-term (working) memory. These two subtests comprise the RBANS Standardized Attention subscale.

Image Acquisition

Imaging was performed on a Siemens 3 tesla Trio with a standard 12-channel head coil (Siemens Medical Solutions, Erlangen, Germany) at the Mellen Center of the Cleveland Clinic. Whole-brain DTI was acquired with monopolar + diffusion weighting gradients [33] and single-shot readout (axial, 102×102 matrix, 255×255 mm Field of View, 75 slices 2.5 mm thick, TE = 76 msec, TR = 9,200 msec, 71 noncollinear diffusion weighting gradients with $b = 1,000 \text{ sec/mm}^2$ and eight

$b = 0$). The achieved signal-to-noise ratio was ~ 13 , with the noise parameter estimated using fit to a noncentral chi distribution [34]. Images were inspected visually for motion, and no evidence of severe motion artifacts was detected. For 12 patients and their matched controls, image acquisition was conducted using an upgraded 32-channel head coil.

Image Analysis

Diffusion-weighted images were first processed using the University of Oxford's Center for Functional Magnetic Resonance Imaging of the Brain (FMRIB) Software Library (FSL), release 5.0 (<https://fsl.fmrib.ox.ac.uk/fsl/fslwiki>) [35]. On the first volume with no gradient ($b = 0$ image), manual checks were performed to search for potential artifacts. No images were found to have artifacts. Eddy current distortions and subject movement were corrected using `eddy_correct`. Next, $b = 0$ volumes were fed into the Brain Extraction Tool (BET) to generate a binary brain mask. These data, along with gradient direction text files, were submitted to FSL DTIfit to fit diffusion tensors to subjects' brain space individually. The output of this step yielded voxel-wise maps of FA, AD (λ_1), and RD (average of λ_2 and λ_3) for each participant.

Statistical Analyses

Self-report and cognitive measures were analyzed with t tests and Wilcoxon rank-sum tests in R 3.6.1 (R Core Team, 2013). All analyses involving DTI parameters were performed using Tract-Based Spatial Statistics (TBSS) [36]. Individual FA maps were nonlinearly transformed into MNI152 standard space by aligning to the FMRIB FA template and averaged across all participants to form a mean FA image. The mean FA image was used to generate a mean FA skeleton at the advised threshold of FA > 0.2, which excluded gray matter and cerebrospinal fluid. These steps were repeated to create mean skeletonized images for the AD, RD, and MD parameters. Using the mean skeletonized images, the Randomise tool was used to extract two sets of regions of significant difference against a null distribution generated from 5,000 random permutations of group membership using Threshold-Free Cluster Enhancement (TFCE) to control for family-wise error. The first set comprised voxels of significant difference between CMI patients and healthy controls on each of the three DTI parameters using t tests. The second set encompassed voxels in which CMI patients and healthy controls differed significantly on each of the DTI parameters after controlling for self-reported chronic pain.

Using the voxel-wise maps of FA, AD, RD, and MD, TBSS was then used to extract a third set of voxel regions in which DTI parameters were significantly correlated with digit symbol coding and digit span performance. Notably, this extraction procedure differed from previous region extraction procedures as it was performed separately for CMI patients and healthy controls using

Table 1. Background measures and neurological characteristics by CMI status

Measure	CM Status		P Value
	CM Patients	Control Participants	
No. of participants	18	18	–
Age, y	33.8 (11.4)	37.3 (14.3)	0.430*
Years of education	14.1 (2.4)	14.2 (2.2)	0.719
Tonsillar position	12.5 (4.6)	1.4 (1.9)	<0.001
No. with syrinx	4	0	–
MPQ pain	28.5 (23.2)	6.1 (11.7)	<0.001
CSP - Headaches	2.9 (1.0)	1.2 (0.7)	<0.001
CSP - Neck pain	2.8 (1.4)	0.7 (0.7)	<0.001
CSP - Arm pain	2.3 (1.5)	0.4 (0.9)	<0.001
CSP - Back pain	2.6 (1.3)	1.2 (1.0)	0.002
CSP - Dizziness	1.9 (1.1)	0.6 (0.6)	<0.001
CSP - Tinnitus	1.9 (1.6)	0.4 (0.8)	0.002
CSP - Difficulty concentrating	2.2 (1.2)	0.9 (0.8)	0.002
CSP - Insomnia	2.3 (1.3)	0.8 (1.1)	<0.001
CSP - Chronic fatigue	2.7 (1.4)	1.1 (0.9)	<0.001
CSP - Irritability	2.2 (1.2)	0.9 (0.8)	0.001
CSP - Forgetfulness	2.1 (1.1)	0.4 (0.7)	<0.001
CSP - Valsalva head pain	2.3 (1.4)	0.1 (0.2)	<0.001
CSP - Generalized body pain	2.2 (1.7)	0.3 (0.7)	<0.001

Values in parentheses indicate standard deviation by group. Bolded values represent group differences in measurement or scale score derived from the Wilcoxon rank-sum test.

CMI = type I Chiari malformation; CSP = Chiari Symptom Profile (scale values correspond the following: 0 = “never,” 1 = “rarely,” 2 = “some of the time,” 3 = “most of the time,” 4 = “all of the time”); MPQ = short-form McGill Pain Questionnaire.

*P values derived from a Student’s *t* test.

the mean skeletonized images that were established within each group (i.e., rather than for the entire sample of CMI patients and healthy controls). Thus, the output of the third set of region extractions comprised distinct voxel regions for which the DTI parameters of CMI patients and controls significantly correlated with the cognitive measures.

Significant voxel regions from the FA, AD, RD, and MD analyses were separately masked using the *fsl-cluster* command. FSL atlas tools and the JHU-ICBM-DTI-81 White Matter Labels were then used to provide standard reference names to identified clusters.

Results

Twenty CMI patients were recruited; however, two CMI patients were not able to tolerate the neuroimaging scan protocols before surgery. Thus, 18 adult CMI patients (1 male) and 18 matched adult healthy controls (1 male) comprised the final sample. Table 1 provides demographic and clinical characteristics of the two groups. Notably, the final sample was well matched for age ($M_{\text{CMI}} = 33.8$ years, $M_{\text{control}} = 37.3$ years) and completed years of education ($M_{\text{CMI}} = 14.1$, $M_{\text{control}} = 14.2$). Additionally, CSP outcomes indicated that the sample of CMI patients exhibited typical symptomatology.

CMI-Related Differences in Diffusion Parameters

FA, RD, and MD analyses all presented clusters of significant difference at $P < 0.05$. Yet, the interpretation of

these group differences was difficult due to the spatially diffuse nature of the clusters. To better specify anatomical associations of clusters and to minimize the likelihood of false discovery, alpha thresholds were lowered by 0.01 in a stepwise fashion until areas of significant difference were better localized or an alpha threshold of 0.01 was reached (Figure 1). For FA, this process resulted in eight white matter clusters of significant group difference in which CMI patients exhibited greater FA compared with healthy controls ($P < 0.03$) (see Table 2 for descriptions). Figure 1 provides representative slices of significant FA clusters. There were no regions in which CMI patients exhibited lower FA than controls.

For RD, CMI patients exhibited lower diffusivity in the left anterior corona radiata compared with controls ($P = 0.019$) (Table 3). Two clusters of significant difference were also identified for MD in the corpus callosum and left superior longitudinal fasciculus (both $P < 0.02$). There were no regions in which CMI patients exhibited greater RD or MD relative to controls. See Figure 2 for representations of significant cluster differences for RD and MD.

No differences were identified for AD in any analyses.

CMI-Related Differences in Diffusion Parameters After Controlling for Pain

For analyses in which clusters of significant difference were identified, group difference analyses were repeated while controlling for chronic pain as reported by the MPQ. After controlling for pain, no group differences in

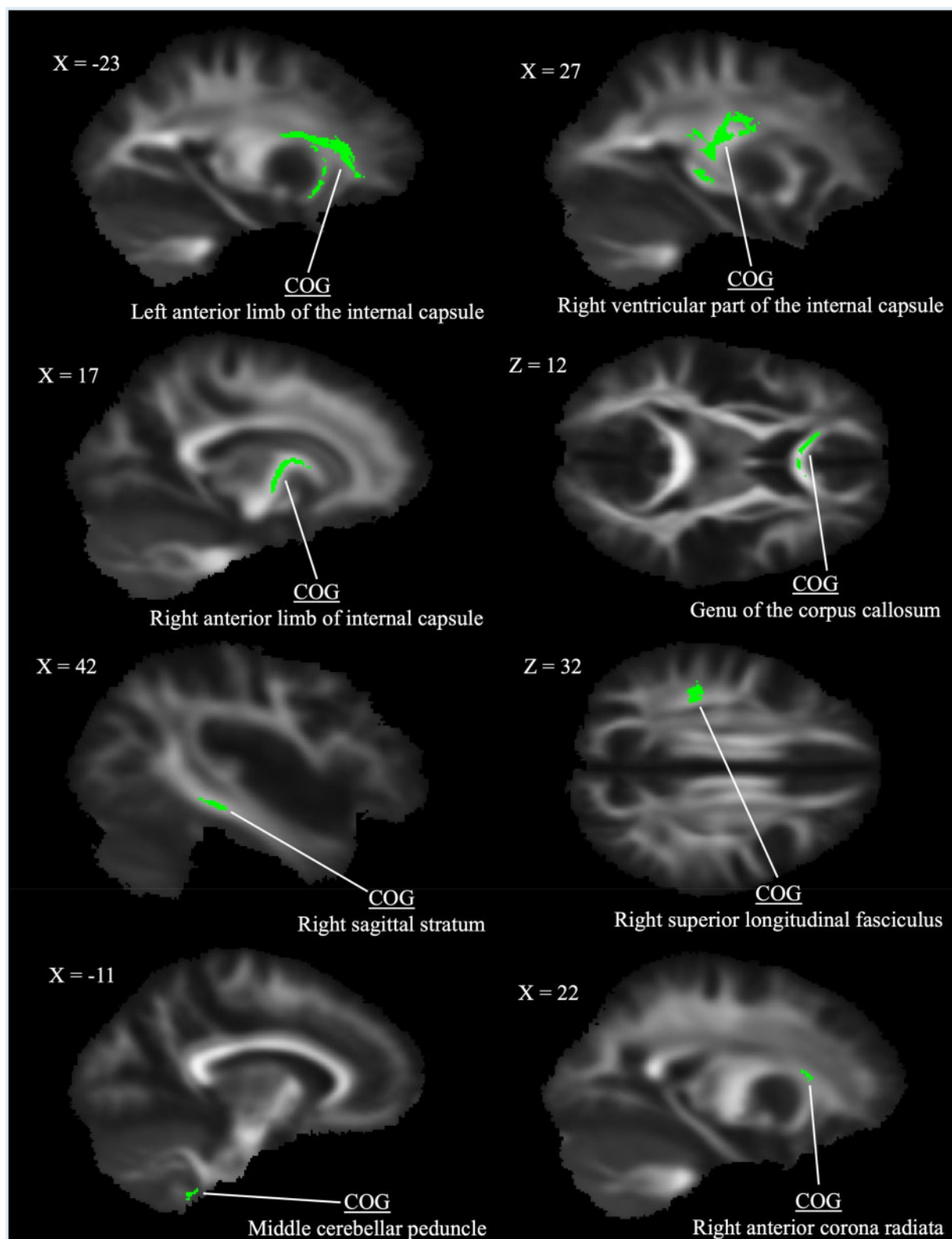


Figure 1. Clusters of significantly greater fractional anisotropy in type I Chiari malformation patients identified using tract-based spatial statistics at $P < 0.03$. Center of gravity identifiers from the Johns Hopkins University white matter labels are provided (see [Table 2](#) for additional cluster descriptions).

FA, RD, or MD were found (all $P > 0.05$). To further confirm these results, an additional set of analyses was performed that identified regions in which FA, RD, and

MD significantly correlated with self-reported pain across both CMI patients and controls. These analyses resulted in several clusters of significant difference (all

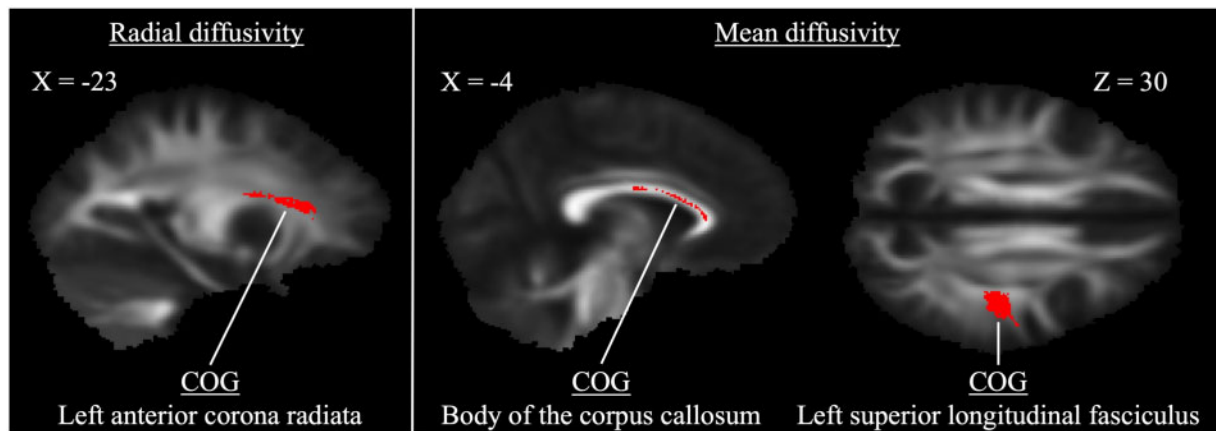


Figure 2. Clusters of significantly lower diffusivity in type I Chiari malformation patients identified using tract-based spatial statistics ($P < 0.01$ for radial diffusivity, $P < 0.02$ for mean diffusivity). Center of gravity identifiers from the Johns Hopkins University white matter labels are provided (see Table 3 for additional cluster descriptions).

Table 2. Group differences in fractional anisotropy between CMI and healthy controls

FA: CMI > Control

Cluster labels	<i>P</i> Value	COG X	COG Y	COG Z
Anterior limb of internal capsule L	0.019	109	146	80
Retroventricular part of the internal capsule R	0.027	61	102	86
Anterior limb of internal capsule R	0.027	74	125	81
Genu of the corpus callosum	0.029	83	152	86
Sagittal stratum R*	0.029	42	94	62
Superior longitudinal fasciculus R	0.028	51	95	104
Middle cerebellar peduncle L*	0.023	101	79	26
Anterior corona radiata R	0.030	68	146	88

Cluster labels reflect Johns Hopkins University (JHU) white matter labels corresponding to the calculated center of gravity for each cluster. All *P* values were corrected for multiple comparisons.

CMI = type I Chiari malformation; COG = center of gravity, calculated as the weighted average of the coordinates by the intensity differences within the cluster.

*Atlas region most closely corresponded to the center of gravity voxel but lay adjacent to the JHU atlas boundary.

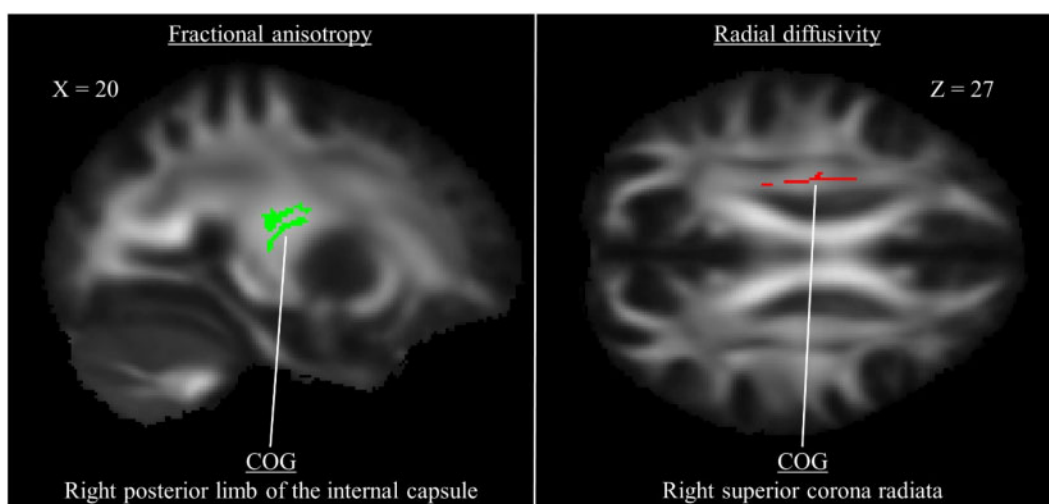


Figure 3. Clusters of significant correlation between diffusion tensor imaging parameters and coding performance in healthy controls. The left figure presents a single cluster in which higher fractional anisotropy was associated with better coding performance. The right figure presents a single cluster in which lower radial diffusivity was associated with better coding performance.

Table 3. Group differences in diffusivity between CMI and healthy controls

RD: CMI < Control				
Cluster Labels	P Value	COG X	COG Y	COG Z
Anterior corona radiata L	0.009	112	146	88
MD: CMI < Control				
Cluster Labels	P Value	COG X	COG Y	COG Z
Body of the corpus callosum*	0.013	95	127	100
Superior longitudinal fasciculus L	0.019	132	103	101

Cluster labels reflect Johns Hopkins University (JHU) white matter labels corresponding to the calculated center of gravity for each cluster. All *P* values were corrected for multiple comparisons.

CMI = type I Chiari malformation; COG = center of gravity, calculated as the weighted average of the coordinates by the intensity differences within the cluster; MD = mean diffusivity; RD = radial diffusivity.

*Atlas region most closely corresponded to the center of gravity voxel but lay adjacent to the JHU atlas boundary.

$P < 0.05$) that closely corresponded to the group differences observed in the primary analyses (Appendices A and B).

Correlations Between Diffusion Parameters and Cognitive Function

CMI patients exhibited lower performance on the RBANS digit symbol coding ($t(34) = -2.26$, $P = 0.030$, $d = 0.75$) and RBANS digit span tasks ($t(34) = -2.40$, $P = 0.022$, $d = 0.80$). In CMI participants, there were no regions in which DTI parameters were significantly correlated with performance on either task. However, in controls, greater FA positively correlated with better coding performance in the right posterior limb of the internal capsule ($P < 0.03$) (Table 4). Additionally, lower RD was negatively correlated with better coding performance in the right superior corona radiata ($P < 0.05$). Representative image slices of these clusters are presented in Figure 3.

Discussion

The aims of the current study were to 1) identify white matter abnormalities between CMI patients and matched healthy controls, 2) determine whether the group differences in white matter abnormalities were independent of chronic pain, and 3) identify whether DTI parameters were significantly correlated with attention. We predicted group differences in measures of anisotropy and diffusivity that would be at least partially dependent on group differences in self-reported chronic pain. We also predicted that we would observe correlations between DTI parameters and cognitive deficits that were independent of pain.

Overall, CMI patients exhibited greater FA and lower MD and RD relative to healthy control participants matched for age, education, and gender. However, there were no longer group differences in FA, MD, and RD after self-reported pain effects were controlled. This suggests that group differences in DTI parameters can be

potentially explained by neural mechanisms associated with the chronic pain response, a perspective that is explored in greater detail below. In addition to these relationships involving pain, healthy controls exhibited two regions of significant correlations between DTI parameters and mental processing speed, as measured with the RBANS coding task. Greater FA in the right posterior internal capsule and lower RD in the right superior corona radiata were associated with improved coding performance. No such association was observed for the CMI group. These results provide preliminary evidence of a weaker association between attention function and DTI in CMI. However, more research is needed to better explore this relationship.

The current results align with the preponderance of the DTI evidence suggesting that FA is increased in adult CMI patients relative to control participants (e.g., anterior brainstem [15], medulla [16]). In contrast, Kumar et al. [14] observed a CMI-related decrease in FA in the genu, splenium, fornix, and putamen in adult CMI patients. One potential explanation of this distinct FA pattern is that Kumar et al. [14] only used 10 gradient directions in their imaging procedure, whereas the other three studies used at least 30 gradient directions (see Jones [37] for issues with using fewer than 15 gradient directions). Additionally, the results of Kumar et al. were based on a small sample (i.e., 10 CMI patients and controls), and, combined with the number of statistical analyses performed, the differences in FA may simply reflect type I error.

Potential Mechanisms Underlying Greater Fractional Anisotropy

Krishna et al. [15] suggested that higher FA levels in CMI are due to an increase in inflammatory compression. In addition to inflammatory compression, unexplored neuronal factors such as decreases in axonal diameter, reductions in cortical volume, or microscopic deficits of axonal structures could potentially contribute to the higher FA values observed in the present study [6,9].

Table 4. Clusters of significant correlation between diffusion parameters and coding in healthy controls

FA: Coding Positively Correlated with FA				
Cluster Labels	<i>P</i> Value	COG X	COG Y	COG Z
Posterior limb of internal capsule R	0.026	65	112	87
RD: Coding Negatively Correlated with RD				
Cluster Labels	<i>P</i> Value	COG X	COG Y	COG Z
Superior corona radiata R	0.042	67	120	100

Cluster labels reflect Johns Hopkins University white matter labels corresponding to the calculated center of gravity for each cluster. All *P* values were corrected for multiple comparisons.

COG = center of gravity, calculated as the weighted average of the coordinates by the intensity differences within the cluster; FA = fractional anisotropy; RD = radial diffusivity.

Astrocyte reactivity at the site of inflammation has also been described and associated with increased FA [38]. Thus, there remain many possibilities regarding the potential mechanisms underlying CMI-specific neuropathology, and more work is needed to determine the viability of the existing hypotheses.

Additionally, as previously described [14], microstructural abnormalities were noted both proximal and distal to the assumed cervico-medullary foci of compression dynamics. These findings suggest that CMI neuropathology should likely be conceived of as a whole-brain phenomenon and not localized to the cerebellum and brainstem. Given the present associations between DTI parameters and self-reported pain, it is noteworthy that recent findings have identified a correlation between noxious pain inhibition and greater FA in connecting pathways along the dorsolateral prefrontal cortex–thalamic tract in healthy individuals subjected to tonic pain [39]. The pain processing system serves as a common indicator of organ injury/dysfunction in a variety of medical disorders, and the present findings suggest that central pain pathways may serve a similar function for the expression of CMI-related neurobiological dysfunction.

Inconsistencies in Measures of Diffusivity

To our knowledge, the present study was also the first to report reduced MD and RD in CMI patients relative to healthy controls. These analyses lie in contrast to the results of two studies that have previously reported diffusivity comparisons in CMI. Kurtcan et al. [16] identified greater apparent diffusion coefficient (ADC) values and AD in the corticospinal tract and medial lemniscus at the level of the medulla oblongata and pons. The authors also identified greater RD in the middle cerebellar peduncles, thalamus, and globus pallidus and greater AD in the genu. In Kumar et al. [14], analyses revealed that areas of significant difference in MD closely corresponded to FA results, with CMI patients exhibiting greater MD in the genu, splenium, fornix, and putamen. Notably, although Krishna et al. [15] reported FA results, the authors did not present any diffusivity analyses.

Thus, including the present study, there appears to be little consistency in diffusivity analyses (for MD, AD, and RD) in CMI. Given the inconsistencies in the diffusivity analyses to date, it is difficult to interpret these results.

Clinical Implications

Although the locus of the DTI effects in CMI are yet to be fully determined, the results of the present study suggest the potential utility of DTI in clinical CMI protocols.

Moreover, given the apparent sensitivity of DTI parameters to pain self-reports, the results also indicate the potential of DTI as an independent marker for pain. DTI also has clear advantages in being able to identify microstructural abnormalities and tissue damage compared with structural MRI [12]. To date, the only study to identify reliable correlations between macrostructural brain abnormalities and symptoms in CMI used a sample that highly overlapped with the present sample [19]. Yet, these macrostructural relationships were few in relation to the entirety of the conducted measurements [26]. In contrast, the present study and Kumar et al. [14] both found associations between DTI measures and behavioral measures, albeit in different directions. In other words, initial findings suggest that DTI may be a more successful method to identify connections between cognitive function and brain structure relative to traditional structural MRI. Though promising, future efforts are needed to examine the viability of DTI as a clinical tool to improve our understanding of factors such as CMI symptom trajectories and the characteristics of optimal surgical candidates.

Limitations

There are four primary limitations to the current study, and the present findings will benefit from future replication. First, while our sample size was an improvement over previous investigations, it remains relatively modest and may be somewhat underpowered for detecting microstructural differences related to CMI. Second, though we took efforts to create highly similar samples of CMI

and control participants, the relatively high levels of education in the current CMI sample may not be representative of the entire CMI population. Third, it should be noted that our imaging analyses and interpretations maintain the inherent limitations of standard DTI imaging studies. These limitations include 1) the inability to calculate heterogeneity of fiber structures within a pixel, 2) the assumption that the largest diffusion axis corresponds to the fiber orientation (i.e., multiple fiber populations cannot be represented at the pixel level), and 3) that participant motion could interfere with the motion of water during the measurement time, lessening the resolution of the resulting image [12]. Finally, although the TBSS approach to image analysis considerably improves on the spatial smoothing problems of VBM approaches, there remains a limitation regarding the interpretation of diffusion measures in regions of crossing fiber tracts [36].

Conclusions

Greater FA and lower RD and MD in several brain regions including the internal capsule, corpus callosum, longitudinal fasciculi, and corona radiata were found to be characteristic of CMI relative to age-, education-, and gender-matched healthy controls. These microstructural white matter differences appear to be related to the self-reported pain and headache that typifies the CMI experience and possibly reflect active inflammatory processes and/or inhibitory pain modulation. In particular, FA and RD also appear to be related to the superior performance on attention tasks observed in healthy control participants and may have implications for the cognitive impairment frequently reported in CMI. Further work is needed to explore these hypotheses and the clinical utility of DTI for improving our understanding of the mechanisms of CMI neuropathology and symptomatology.

Acknowledgments

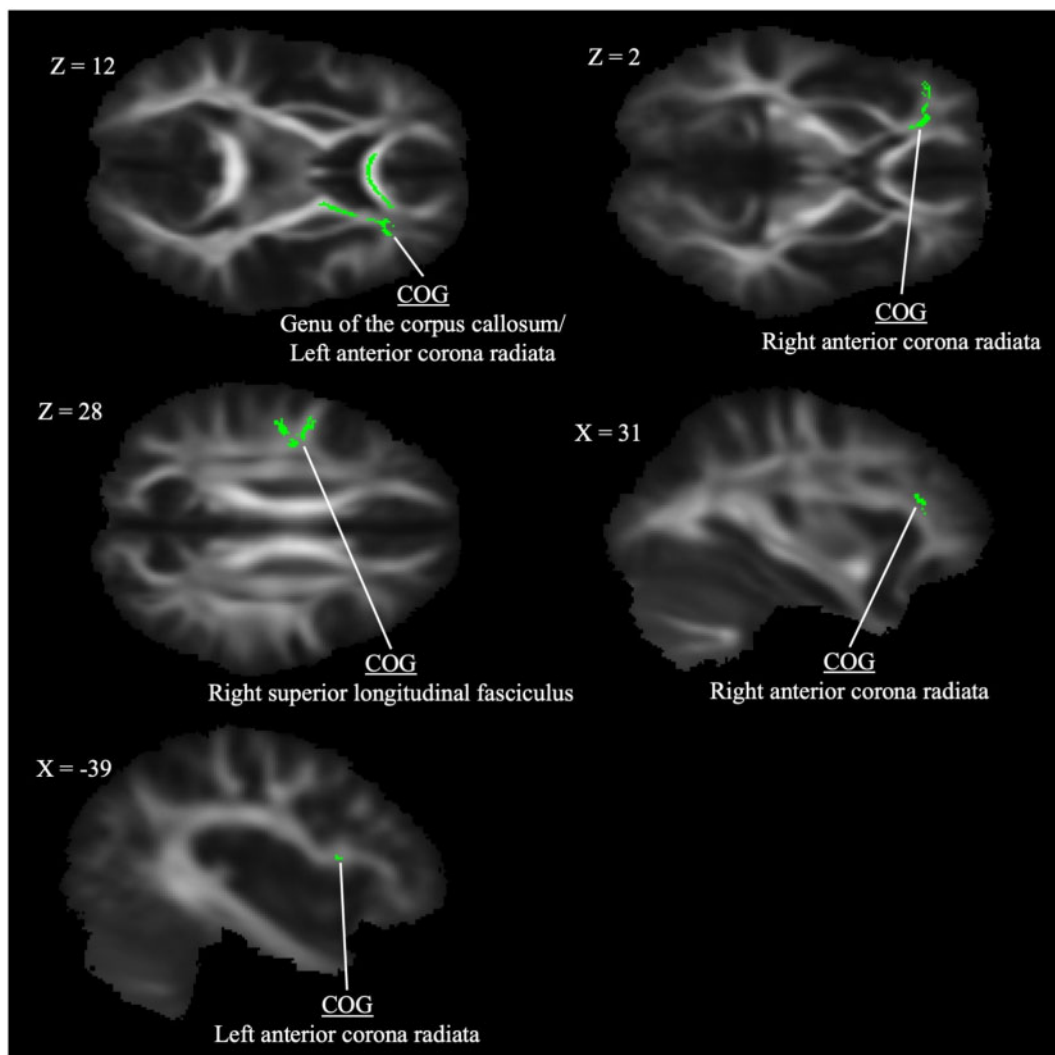
We gratefully acknowledge the support of Thorsten Feiweir of Siemens Healthcare for use of the advanced diffusion works-in-progress package.

References

- Fischbein R, Saling J, Marty P, et al. Patient-reported Chiari malformation type I symptoms and diagnostic experiences: A report from the national Conquer Chiari Patient Registry database. *Neurol Sci* 2015;36(9):1617–24.
- Milhorat TH, Chou MW, Trinidad EM, et al. Chiari I Malformation redefined: Clinical and radiographic findings for 364 symptomatic patients. *Neurosurgery* 1999;44(5):1005–17.
- Furuya K, Sano K, Segawa H, et al. Symptomatic tonsillar ectopia. *J Neurol Neurosurg Psychiatry* 1998;64:221–6.
- Meadows J, Kraut M, Guarnieri M, et al. Asymptomatic Chiari type I malformations identified on magnetic resonance imaging. *J Neurosurg* 2000;92(6):920–6.
- Strahle J, Muraszko K, Kapurch J, et al. Chiari malformation type I and syrinx in children undergoing magnetic resonance imaging. *J Neurosurg Pediatr* 2011;8:205–13.
- Concha L. A macroscopic view of microstructure: Using diffusion-weighted images to infer damage, repair, and plasticity of white matter. *Neuroscience* 2014;276:14–28.
- Wakana S, Jiang H, Nagae-Poetscher L, et al. Fiber tract-based atlas of human white matter anatomy. *Radiology* 2004;230(1):77–87.
- Peters A. The effects of normal aging on myelin and nerve fibers: A review. *J Neurocytol* 2002;31(8/9):581–93.
- Beaulieu C. The basis of anisotropic water diffusion in the nervous system – a technical review. *NMR Biomed* 2002;15(7–8):435–55.
- Bihan D, Mangin J, Poupon C, et al. Diffusion tensor imaging: Concepts and applications. *J Magn Reson Imaging* 2001;13:534–46.
- Inglese M, Bester M. Diffusion imaging in multiple sclerosis: Research and clinical implications. *NMR Biomed* 2010;23(7):865–72.
- Mori S, Zhang J. Principles of diffusion tensor imaging and its applications to basic neuroscience research. *Neuron* 2006;51(5):527–39.
- Song S-K, Yoshino J, Le T, et al. Demyelination increases radial diffusivity in corpus callosum of mouse brain. *Neuroimage* 2005;26(1):132–40.
- Kumar M, Rathore R, Srivastava A, et al. Correlation of diffusion tensor imaging metrics with neurocognitive function in Chiari I malformation. *World Neurosurg* 2011;76(1–2):189–94.
- Krishna V, Sammartino F, Yee P, et al. Diffusion tensor imaging assessment of microstructural brainstem integrity in Chiari malformation type I. *J Neurosurg* 2016;125(5):1112–9.
- Kurtcan S, Alkan A, Yetis H, et al. Diffusion tensor imaging findings of the brainstem in subjects with tonsillar ectopia. *Acta Neurol Belg* 2018;118(1):39–45.
- Assaf Y, Ben-Sira L, Constantini S, et al. Diffusion tensor imaging in hydrocephalus: Initial experience. *Am J Neuroradiol* 2006;27(8):1717–24.
- Dworkin RH, Turk DC, Revicki DA, et al. Development and initial validation of an expanded and revised version of the short-form McGill Pain Questionnaire (SF-MPQ-2). *Pain* 2009;144(1):35–42.
- Houston JR, Allen PA, Rogers JM, et al. Type I Chiari malformation, RBANS performance, and brain morphology: Connecting the dots on cognition and macro-level brain structure. *Neuropsychology* 2019;33(5):725–38.
- Garcia M, Allen PA, Li X, et al. An examination of pain, disability, and the psychological correlates of Chiari malformation pre- and post-surgical correction. *Disabil Health J* 2019;12:649–56.
- Allen PA, Delahanty D, Kaut KP, et al. Chiari 1000 Registry Project: Assessment of surgical outcome on self-focused attention, pain, and delayed recall. *Psychol Med* 2018;48(10):1634–43.
- Bushnell CM, Čeko M, Low LA. Cognitive and emotional control of pain and its disruption in chronic pain. *Nat Rev Neurosci* 2013;14(7):502–11.
- García M, Amayra I, Lázaro E, et al. Comparison between decompressed and non-decompressed Chiari malformation type I patients: A neuropsychological study. *Neuropsychologia* 2018;121:135–43.
- García M, Lázaro E, López-Paz J, et al. Cognitive functioning in Chiari malformation type I without posterior fossa surgery. *Cerebellum* 2018;17(5):564–74.
- Lacy M, Parikh S, Costello R, et al. Neurocognitive functioning in unoperated adults with Chiari malformation type I. *World Neurosurg* 2019;126:e641–5.

26. Rogers JM, Savage G, Stoodley MA. A systematic review of cognition in Chiari I malformation. *Neuropsychol Rev* 2018;28(2):176–87.
27. Allen PA, Houston JR, Pollock JW, et al. Task-specific and general cognitive effects in Chiari malformation type I. *PLoS One* 2014;9(4):e94844.
28. Houston JR, Hughes ML, Lien M-C, et al. An electrophysiological study of cognitive and emotion processing in type I Chiari malformation. *Cerebellum* 2018;17(4):404–18.
29. Melzack R. The short-form McGill Pain Questionnaire. *Pain* 1987;30(2):191–7.
30. Mueller D, Oro' J. The Chiari Symptom Profile: Development and validation of a Chiari/syringomyelia-specific questionnaire. *J Neurosci Nurs* 2013;45(4):205–10.
31. Randolph C, RBANS U. Repeatability Battery for the Assessment of Neuropsychological Status. Bloomington, MN: NCS Pearson; 2012.
32. Randolph C, Tierney M, Mohr E, et al. The Repeatability Battery for the Assessment of Neuropsychological Status (RBANS): Preliminary clinical validity. *J Clin Exp Neuropsychol* 1998;20(3):310–9.
33. Morelli J, Runge V, Kirsch J, et al. Evaluation of a modified Stejskal-Tanner diffusion encoding scheme, permitting a marked reduction in TE, in diffusion-weighted imaging of stroke patients at 3T. *Invest Radiol* 2010;45:29–35.
34. Sakaie K, Lowe M. Retrospective correction of bias in diffusion tensor imaging arising from coil combination mode. *Magn Reson Imaging* 2017;37:203–208.
35. Smith S, Jenkinson M, Woolrich MW, et al. Advances in functional and structural MR image analysis and implementation as FSL. *Neuroimage* 2004;23:S208–19.
36. Smith S, Jenkinson M, Johansen-Berg H, et al. Tract-based spatial statistics: Voxelwise analysis of multi-subject diffusion data. *Neuroimage* 2006;31(4):1487–505.
37. Jones D. The effect of gradient sampling schemes on measures derived from diffusion tensor MRI: A Monte Carlo study. *Magn Reson Med* 2004;51(4):807–15.
38. Budde MD, Janes L, Gold E, et al. The contribution of gliosis to diffusion tensor anisotropy and tractography following traumatic brain injury: Validation in the rat using Fourier analysis of stained tissue sections. *Brain* 2011;134(8):2248–60.
39. Lin RL, Douaud G, Filippini N, et al. Structural connectivity variances underlie functional and behavioral changes during pain relief induced by neuromodulation. *Sci Rep* 2017;7(1):41603.

Appendix A. Clusters of significant correlation between fractional anisotropy and MPQ pain



Clusters of significant positive correlation between FA and MPQ pain across all participants.

FA: MPQ Pain Positively Correlated with FA

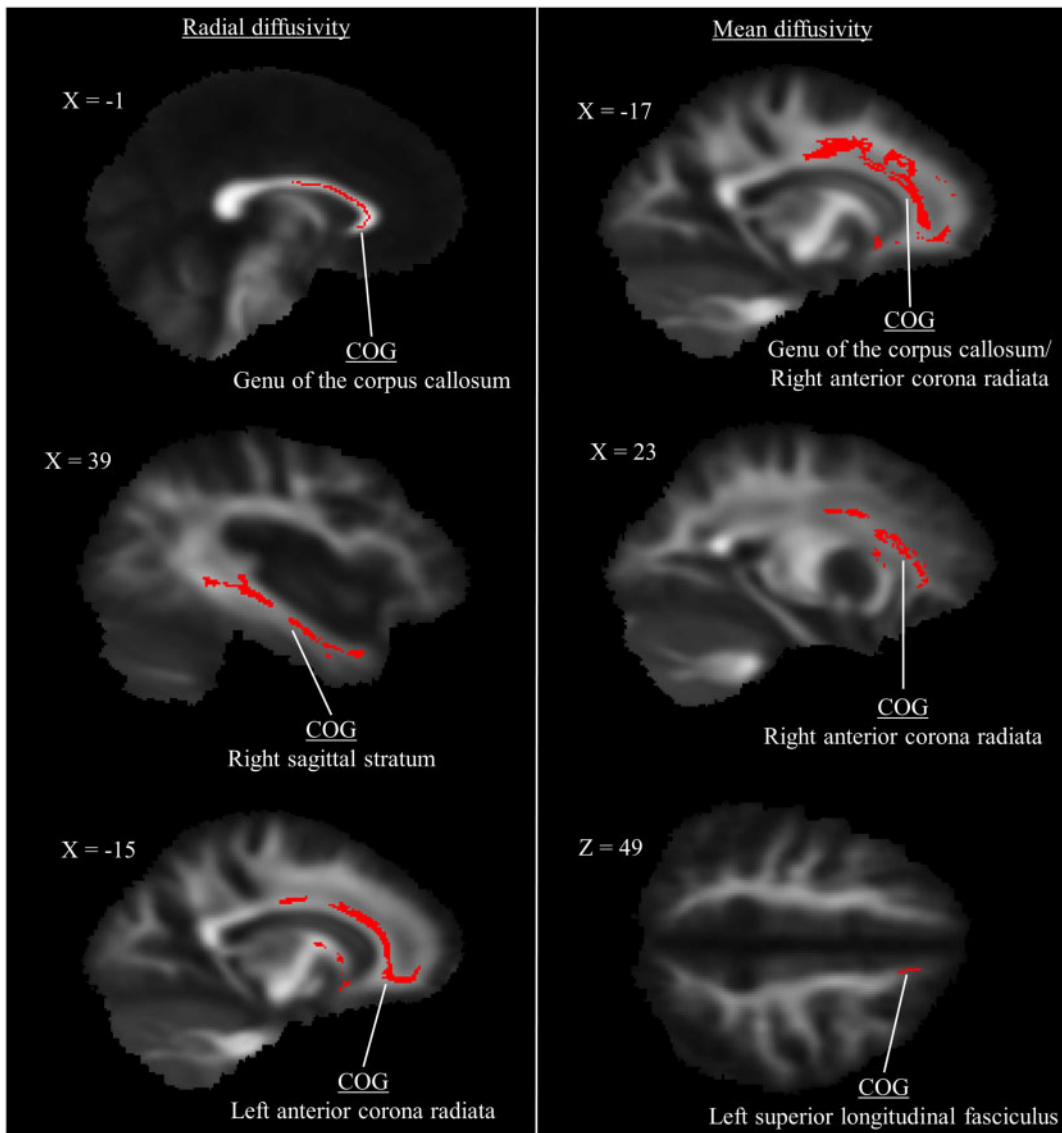
Cluster Labels	P Value	COG X	COG Y	COG Z
Genu of the corpus callosum/anterior corona radiata L*	0.016	100	144	86
Anterior corona radiata R	0.024	63	151	87
Superior longitudinal fasciculus R*	0.027	47	116	102
Anterior corona radiata R*	0.029	58	161	93
Anterior corona radiata L*	0.030	129	141	85

Cluster labels reflect Johns Hopkins University (JHU) white matter labels corresponding to the calculated center of gravity for each cluster. All P values were corrected for multiple comparisons.

COG = center of gravity, calculated as the weighted average of the coordinates by the intensity differences within the cluster; FA = fractional anisotropy; MPQ = McGill Pain Questionnaire.

*Atlas region most closely corresponded to the center of gravity voxel but lay adjacent to the JHU atlas boundary.

Appendix B. Clusters of significant correlation between diffusion parameters and MPQ pain



Clusters of significant negative correlation between diffusion parameters and MPQ pain across all participants. The left column presents results for radial diffusivity, and the right column presents results for mean diffusivity.

 RD: MPQ Pain Negatively Correlated with RD

Cluster Labels	<i>P</i> Value	COG X	COG Y	COG Z
Genu of the corpus callosum	0.012	91	146	89
Sagittal stratum R	0.025	52	107	65
Anterior corona radiata L*	0.029	119	173	76

 MD: MPQ Pain Negatively Correlated with MD

Cluster Labels	<i>P</i> Value	COG X	COG Y	COG Z
Genu of the corpus callosum/anterior corona radiata R*	0.014	112	145	90
Anterior corona radiata R	0.019	68	152	90
Superior longitudinal fasciculus L	0.020	99	149	124

Cluster labels reflect Johns Hopkins University (JHU) white matter labels corresponding to the calculated center of gravity for each cluster. All *P* values were corrected for multiple comparisons.

COG = center of gravity, calculated as the weighted average of the coordinates by the intensity differences within the cluster; MD = mean diffusivity; RD = radial diffusivity.

*Atlas region most closely corresponded to the center of gravity voxel but lay adjacent to the JHU atlas boundary.